Journal of Hydrology: Regional Studies 2 (2014) 35–48

Contents lists available at ScienceDirect

Journal of Hydrology: Regional Studies

journal homepage: www.elsevier.com/locate/ejrh

Multivariate power-law models for streamflow prediction in the Mekong Basin

Guillaume Lacombe [a,*], Somphasith Douangsavanh [a], Richard M. Vogel [b], Matthew McCartney [a], Yann Chemin [c], Lisa-Maria Rebelo [a], Touleelor Sotoukee [a]

[a] International Water Management Institute, Southeast Asia Regional Office, PO Box 4199, Vientiane, Lao Democratic People's Republic
[b] Tuft University, Department of Civil and Environmental Engineering, Medford, MA 02155, USA
[c] International Water Management Institute, Headquarters, PO Box 2075, Colombo, Sri Lanka

ARTICLE INFO

Article history:
Received 7 March 2014
Received in revised form 8 August 2014
Accepted 13 August 2014

Keywords:
Streamflow prediction
Ungauged catchment
Multivariate regression models
Mekong

ABSTRACT

Study region: Increasing demographic pressure and economic development in the Mekong Basin result in greater dependency on river water resources and increased vulnerability to streamflow variations.

Study focus: Improved knowledge of flow variability is therefore paramount, especially in remote catchments, rarely gauged, and inhabited by vulnerable populations. We present simple multivariate power-law relationships for estimating streamflow metrics in ungauged areas, from easily obtained catchment characteristics. The relations were derived from weighted least square regression applied to streamflow, climate, soil, geographic, geomorphologic and land-cover characteristics of 65 gauged catchments in the Lower Mekong Basin. Step-wise and best subset regressions were used concurrently to maximize the prediction *R*-squared computed by leave-one-out cross-validations, thus ensuring parsimonious, yet accurate relationships.

New hydrological insights for the region: A combination of 3–6 explanatory variables – chosen among annual rainfall,

* Corresponding author. Tel.: +856 21 77 14 38.
E-mail addresses: g.lacombe@cgiar.org (G. Lacombe), s.douangsavanh@cgiar.org (S. Douangsavanh), richard.vogel@tufts.edu (R.M. Vogel), m.mccartney@cgiar.org (M. McCartney), ychemin@gmail.com (Y. Chemin), l.rebelo@cgiar.org (L.-M. Rebelo), t.sotoukee@cgiar.org (T. Sotoukee).

http://dx.doi.org/10.1016/j.ejrh.2014.08.002

drainage area, perimeter, elevation, slope, drainage density and latitude – is sufficient to predict a range of flow metrics with a prediction *R*-squared ranging from 84 to 95%. The inclusion of forest or paddy percentage coverage as an additional explanatory variable led to slight improvements in the predictive power of some of the low-flow models (lowest prediction *R*-squared = 89%). A physical interpretation of the model structure was possible for most of the resulting relationships. Compared to regional regression models developed in other parts of the world, this new set of equations performs reasonably well.

1. Introduction

Population growth, economic development and climate change increase the vulnerability of people and ecosystems to variations in river flow. The Mekong Basin in Southeast Asia exemplifies these issues with growing irrigation water demand (Pech and Sunada, 2008), greater flood-risk exposure (Osti et al., 2011), and hydropower-induced changes in seasonal river flow and ecology (Arias et al., 2012; Ziv et al., 2012). Adaptation measures are hampered by uncertainties in projected streamflow changes (Kingston et al., 2011). A number of hydrological models have been developed for the Mekong Basin to predict streamflow variability, however their complexity and lack of transparency (Johnston and Kummu, 2012), often limit possible users to modeling experts, instead of the practitioners working closely with populations affected by flow extremes. Additionally, the majority of models have been developed to predict flow along the Mekong mainstem, precluding accurate assessments in headwater catchments where populations are repeatedly exposed to flash floods and/or water resource shortages.

Flow duration curves (FDCs) provide an integrated representation of flow variability that can be used for water resource planning, storage design and flood risk management (Castellarin et al., 2013). A period-of-record FDC indicates the percentage of time (duration) a particular value of streamflow is exceeded over a historical period. Similarly, a median annual FDC can reflect the percentage of time a particular value of streamflow is exceeded in a typical or median year (see Vogel and Fennessey, 1994). Various parametric and nonparametric statistical methods exist to predict an FDC in ungauged catchments and have been applied in many parts of the world (Castellarin et al., 2004).

We present a set of new multivariate power-law models to predict FDC percentiles as well as other flow metrics, at any location along the tributaries of the Lower Mekong River (Fig. 1) using easily determined catchment characteristics. Section 2 describes the main steps of the multiple regression analysis. Section 3 presents the data used to empirically develop the models. Section 4 presents the equations of the power-law models, discusses their significance and compares their performance with other case studies.

2. Multiple regression analysis

We used a multivariate power-law equation (Eq. (1)), already used in many parts of the world (Vogel et al., 1999; Castellarin et al., 2004), to estimate the river flow Q from m catchment characteristics X_i ($i = 1, \ldots, m$). A logarithmic transformation of Eq. (1) results in a log-linear model (Eq. (2)) whose coefficients β_i ($i = 1, \ldots, m$) can be determined by multiple linear regression.

$$Q = \exp^{\beta_0} \cdot X_1^{\beta_1} \cdot X_2^{\beta_2} \cdots X_m^{\beta_m} \cdot \nu \tag{1}$$

$$\ln(Q) = \beta_0 + \beta_1 \cdot \ln(X_1) + \beta_2 \cdot \ln(X_2) + \cdots + \beta_m \cdot \ln(X_m) + \varepsilon \tag{2}$$

β_0 is the intercept term of the model. ν (Eq. (1)) and ε (Eq. (2)) are the log-normally and normally distributed errors of the models, respectively. The natural logarithm (ln) being defined for strictly positive values only, catchment characteristics X_i and flow Q with possible zero values are incremented

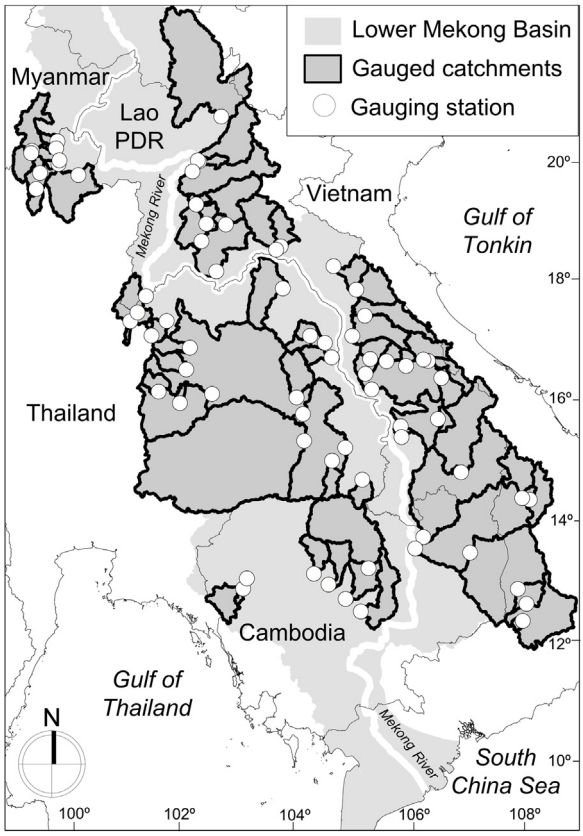

Fig. 1. Location of the 65 gauging stations and their catchments in the Lower Mekong River Basin.

by one prior to being used in the regression analysis (Homa et al., 2013). In these cases, X_i and/or Q should be replaced by $X_i + 1$ and/or $Q + 1$, respectively, in Eqs. (1) and (2). The selection of the explanatory variables X_i, and the calculation of their respective coefficients β_i, is performed by weighted least squares regressions applied to n observations Q_j ($j = 1, \ldots, n$) of Q and their respective m catchment characteristics X_{ij}. A description of the approaches used to obtain the dependent variables Q_j and the independent variables X_{ij} is presented in Section 3. Unlike ordinary least square regressions treating the n observations of Q_j equally, weighted least square regression (Tasker, 1980) enables the varying number k_j of hydrological years used to calculate each flow statistic Q_j and its associated climate characteristics to be taken into account. Values of Q_j derived from a greater number of hydrological years are more precise (have lower variance) and thus should have a greater weight in the regression. However, this reliability decreases as the variance of Q_j increases. To account for these two counteracting factors, weights (w_j) were calculated as follows:

$$w_j = \frac{\sqrt{k_j}}{Stdev(Q_j)} \tag{3}$$

where $Stdev(Q_j)$ is the standard deviation of Q_j. If Q_j is the annual flow, w_j can be interpreted as the inverse of the standard deviation of a mean Q_j estimated from k_j years. In this case, w_j is the exact weight for the sample mean but is only an approximation of the weight for all other streamflow metrics presented in Section 3.1.

The selection of the best set of explanatory variables X_i in Eq. (2) was guided by the combined use of the selection algorithms knows as "best subsets regression" and "step-wise regression" both of which are widely available in statistical packages. This selection was intended to maximize the prediction R-squared (R^2_{pred}) calculated by leave-one-out cross-validations. Unlike the classical R-squared the maximization of which can lead to model over-fitting and loss of robustness, R^2_{pred} reflects the ability of the model to predict observations which were not used in the model calibration. Maximizing R^2_{pred} generally leads to greater parsimony in the number of explanatory variables. An explanatory variable was considered to be statistically significantly different from zero if its p-value, derived from Student's t test, was lower than 0.05. The required homoscedasticity (homogeneity of variance) of the model residuals ε was verified by visual inspection of the residual plots. Possible multi-collinearity among the explanatory variables was controlled with the variance inflation factor (VIF) which should never exceed 8. VIFs for all explanatory variables of our models were found to never and rarely exceed 3 and 2, respectively. The influence statistic Cooks D (Cook and Weisberg, 1982) was used to identify and remove outlier catchments exhibiting high influence on the estimation of the model coefficients. Removal of these outliers (between 2 and 5, depending on the flow metrics) was found to systematically increase the performance of the models (see Helsel and Hirsch, 2002 for further background on R-squared, VIF and influence statistics). The predictive power of the model was measured by four performance criteria whose values are provided in Table 3: the adjusted R-squared (R^2_{adj}), R^2_{pred}, the Nash–Sutcliffe efficiency coefficients (NSE) and the root mean square normalized error (RMSNE). While R^2_{pred} indicates how well the model predicts responses to new observations, R^2_{adj} is a useful tool for comparing the explanatory power of models with different numbers of predictors. Unlike the classical R-squared whose value increases when a new predictor is added, R^2_{adj} will increase only if the new term improves the model more than would be expected by chance. A value of R^2_{adj} much greater than R^2_{pred} indicates that one or more observations are exerting too much influence on the accuracy of the regression. Thus, this comparison can help to control for the effect of removing outliers on the model performance and can be used concurrently with the statistic Cooks D. In addition, R^2_{adj} values are useful to compare our results with other studies. While R^2_{adj} and R^2_{pred} are squared correlation coefficients measuring the linear association between observations and predictions, NSE measures the goodness of fit of linear or non-linear models (e.g. power law models), thus allowing performance comparison with any hydrological model. RMSNE is a common error measure for estimators, combining both the bias and the dispersion component of the error. NSE and RMSNE are computed as follows:

$$\mathrm{NSE} = 1 - \frac{\sum_j (Q_{j,pred} - Q_{j,obs})^2}{\sum_j (Q_{j,obs} - \overline{Q_{obs}})^2} \tag{4}$$

$$\mathrm{RMSNE} = \sqrt{\frac{1}{n} \times \sum_j \left(\frac{Q_{j,pred} - Q_{j,obs}}{Q_{j,obs}} \right)^2} \tag{5}$$

where $Q_{j,pred}$ and $Q_{j,obs}$ are the predicted and observed flow in the catchment j, respectively, and $\overline{Q_{obs}}$ is the spatial mean of the observed flow among all studied catchments. Finally, it should be noted that bias corrections, often required when fitting a model by linear regression on a transformed scale, were found not to improve our results and thus are not presented here.

3. Data preparation

The power law models were developed using hydrological data and 17 catchment characteristics (listed in Table 2) from a set of 65 gauged catchments in the Lower Mekong Basin (Fig. 1). This section explains how these catchments were selected and how their flow metrics and characteristics (i.e. candidate explanatory variables) were computed.

3.1. Streamflow

The streamflow dataset used comprises records of daily discharge at 71 sites located along the tributaries of the Lower Mekong River. This dataset was prepared and provided by the Mekong River Commission (MRC). 65 stations located along 50 rivers were selected for our study (Fig. 1), on the basis that they provide records which were not subject to dam regulation, gaps, and questionable values. At each station, the selected streamflow time series include between 1 and 41 years of records with a median value of 17 years. Records are available between January 1951 and December 2007. Flow percentiles at each station were computed following the method suggested by Vogel and Fennessey (1994): an annual FDC was derived from each period of continuous record during a hydrological year (April 1st–March 31st). A median annual FDC was computed using all year-specific annual FDCs. Compared to the more classical period-of-record FDC, the median annual FDC has the advantage of not being sensitive to outliers and being less sensitive to the particular period of record used. Eleven flow percentiles (i.e. exceedance probabilities) were selected and obtained from the FDC: 0.05, 0.10, 0.20, 0.30, 0.40, 0.50, 0.60, 0.70, 0.80, 0.90 and 0.95. Additionally, we computed the median of the annual minimum, maximum and mean flow (referred to as Min, Max and Mean, respectively, in Table 3). These 14 flow metrics are the dependent variables Q (Eqs. (1) and (2)) that we aimed to predict with the power-law models. Since daily flow values below 1 $m^3 s^{-1}$ are not provided in the MRC data base, regression models had to be computed using catchments with median values of flow percentiles greater than 1 $m^3 s^{-1}$. This resulted in the removal of 15, 11, 10, 7 and 5 catchments from the datasets used to compute the Min, 0.95, 0.90, 0.80 and 0.70 flow percentiles, respectively.

3.2. Rainfall

The high-resolution ($0.25^\circ \times 0.25^\circ$) daily gridded precipitation database "Aphrodite" (Yatagai et al., 2012), freely available at http://www.chikyu.ac.jp/precip/was used to compute daily time series (1951–2007) of areal rainfall over the selected catchments. Gridded values lying within a catchment were averaged, accounting for the reduced size of cells that overlap the catchment boundary. Several rainfall variables were tested for correlation with each of the 14 studied flow variables: annual and monthly rainfall depths, rainfall depth cumulated over the l-day rainiest periods of the hydrological year ($l = 5$, 10, and 15). Among the explanatory variables considered, annual rainfall was found to exhibit the greatest correlation coefficients with all of the 14 flow variables. Hence, it was included as the only candidate explanatory rainfall variable for the power-law models (Table 2). Median rainfall and median flow values used in the regression analyses were derived from the same hydrological years.

3.3. Geomorphological and geographic characteristics

Using standard algorithms available in ArcMap 10.0, several geomorphological catchment characteristics, likely to influence hydrology, were derived from HydroSHEDS, a quality-controlled 90-m digital elevation model (Lehner et al., 2006) freely available at http://hydrosheds.cr.usgs.gov/index.php. These characteristics include drainage area, perimeter, mean slope, mean elevation, drainage density and drainage direction. The drainage density is the cumulative length of all streams within the catchment, normalized by the drainage area of the catchment. The stream network consists of all outlet points draining an area greater than 40 km^2. This threshold value was selected so as to best capture the variability of drainage densities among the studied catchments. Four variables representing mean drainage directions were calculated, namely South, Southwest, West and Northwest. A value of 1 (or 0) means that the catchment is draining toward the named direction (or opposite to the named direction). The geographic coordinates of the flow gauging stations (latitude and longitude) were selected as two additional candidate explanatory variables (Table 2).

3.4. Soil characteristics

Two soil characteristics, likely to control hydrological processes, were selected from the MRC soil database (MRC, 2011): soil depth and top soil texture. A four-unit scale suggested by MRC was used

Table 1
The 4-unit scale of the two soil characteristics.

	Soil depth	Top soil texture
1	<30 cm	Coarse
2	30–50 cm	Medium
3	30–50 cm with gravel	Fine
4	>50 cm	Peat

Table 2
List of the candidate explanatory variables (catchment characteristics) used in the multiple regression analyses.

Variable Name	Definition	Unit	Minimum value	Median value	Maximum value
Climatic characteristics					
Rain	Median annual rainfall	mm/year	880	1416	2093
Geomorphologic characteristics					
Area	Drainage area	km^2	207	3278	106,748
Peri	Perimeter	km	76	401	2090
Slop	Mean slope	%	2	15	32
Elev	Mean elevation	m	84	562	1168
Drai	Drainage density = total stream lengths/drainage area	km^{-1}	0.09	0.13	0.17
S	Ratio of area draining south	%	21	37	45
SW	Ratio of area draining southwest	%	26	44	62
W	Ratio of area draining west	%	16	35	52
NW	Ratio of area draining northwest	%	28	41	51
Geographic characteristics (coordinates of the flow gauging stations)					
Lati	Latitude	decimal degree	12.33	16.70	20.70
Long	Longitude	decimal degree	99.35	104.03	108.00
Soil characteristics (averaged over catchment area)					
Sdep	Mean soil depth	4-unit scales	0.00	3.07	4.00
Sste	Mean top soil texture	4-unit scales	0.00	2.08	2.91
Land cover characteristics (ratio of catchment area coverage)					
Fore	Forest	%	3	75	98
Padd	Paddy	%	0	4	77
Wetl	Wetlands (marsh and swamp)	%	0	0	1.23

for quantification (Table 1). Averaged values for each soil characteristics and each catchment were averaged by weighting each scale unit by the respective area covered in the catchment.

3.5. Land cover

Three land-cover types, likely to alter hydrology, were selected as candidate explanatory variables: forest, bunded rainfed lowland rice paddy fields, the majority of which is never irrigated, and wetlands, including marsh and swamp. The percentage of surface area covered by each land-cover type in each catchment was computed using the digitized 2003 land cover map of the Lower Mekong Basin prepared by MRC (2011). Forest cover was produced by merging four forest types available as separate land-cover classes in the published map: “coniferous forest”, “deciduous forest”, “evergreen forest” and “forest plantation”. The two other land-cover types were directly available since they correspond to distinct land cover classes on the published map.

4. Results and discussion

Table 3 presents the results of the multiple regression analyses for the 14 flow metrics listed in column 1. Column 2 provides the value of the intercept term β_0. Columns 3–11 provide the coefficients β_t associated with each explanatory variable X_i included in the power-law models (cf. Eq. (1)). Units

Table 3
Parameters of the power-law models. Column 1: estimated flow metrics (cf. Section 3.1). Columns 2–11: coefficients and t-ratios (in parentheses) of the explanatory variables (cf. Table 2 for description of the variables). Column 12: performance of the models (%) measured by R^2_{adj} (top-left value), R^2_{pred} (top-right value), NSE (bottom-left value) and RMSNE (bottom-right value) (cf. Section 4 for description of these performance criteria).

Q (m^3/s)	β_0	Explanatory variables (β_i, $i>0$)									Performance	
		Rain	Peri	Elev	Area	Drai	Slop	Lati	Padd	Fore		
Max		1.870		−0.796	0.668	2.694	0.798	−1.423			90.4	89.1
		(11.62)		(−3.96)	(14.78)	(4.66)	(5.08)	(−2.65)			86.2	71.5
0.05	−14.434	2.376			0.862	2.016					94.6	94.1
	(−6.31)	(10.21)			(21.25)	(3.81)					89.1	53.1
0.10	−21.435	2.608			0.970						93.9	93.5
	(−13.31)	(11.81)			(27.37)						89.4	55.3
0.20	−23.087	2.742			0.988						94.7	94.3
	(−14.07)	(11.94)			(28.89)						92.1	54.7
0.30	−24.135	2.519		0.335	0.992						92.5	91.8
	(−12.34)	(9.51)		(3.34)	(23.20)						92.3	56.6
0.40	−29.234	2.603	1.789	0.566							93.2	92.5
	(−15.53)	(10.45)	(24.90)	(5.82)							89.3	51.7
0.50	−32.293	2.748	1.792	0.807							92.4	91.7
	(−15.95)	(10.15)	(23.03)	(7.92)							84.6	54.4
	−31.247	2.529	1.798	0.714						0.262	92.8	92.1
	(−15.38)	(8.92)	(23.75)	(6.57)						(2.08)	85.2	53.1
0.60	−27.435	2.582	1.558	1.145				−1.650			92.6	91.9
	(−12.27)	(10.10)	(20.86)	(10.33)				(−3.29)			82.7	57.7
	−24.521	2.289	1.600	0.963				−1.526	−0.155		93.3	92.4
	(−10.13)	(8.48)	(21.87)	(7.56)				(−3.17)	(−2.56)		87.7	57.1
0.70	−27.047	2.586	1.440	1.272				−1.935			91.1	90.1
	(−10.54)	(8.89)	(18.23)	(10.83)				(−3.64)			79.7	62.1
	−24.023	2.307	1.469	1.074				−1.820	−0.155		91.9	90.7
	(−8.78)	(7.70)	(19.26)	(7.80)				(−3.58)	(−2.49)		85.3	56.8
0.80	−29.130	2.909	1.373	1.309				−2.034			92.0	91.0
	(−10.99)	(9.77)	(17.98)	(11.30)				(−3.97)			77.9	71.9
	−25.761	2.582	1.411	1.080				−1.852	−0.189		93.2	92.2
	(−9.67)	(8.81)	(19.78)	(8.38)				(−3.90)	(−3.16)		85.0	64.2

Table 3 (*Continued*)

Q (m^3/s)	β_0	Explanatory variables (β_i, $i>0$)									Performance	
		Rain	Peri	Elev	Area	Drai	Slop	Lati	Padd	Fore		
0.90	−28.562	2.613	1.467	0.844		−1.706	0.587	−2.503			90.9	89.5
	(−7.21)	(7.19)	(15.45)	(3.67)		(−2.13)	(2.97)	(−4.51)			77.2	87.2
0.95	−29.536	3.003	1.312	1.354				−2.236			86.4	84.1
	(−8.83)	(7.98)	(13.52)	(9.92)				(−4.01)			75.6	86.1
	−27.857	2.698	1.436	0.966				−1.291	−0.285		91.6	90.5
	(−9.95)	(8.70)	(16.35)	(7.30)				(−2.59)	(−4.43)		84.0	79.0
Min	−32.951	3.027	1.416	0.803		−2.684	0.535	−2.598			90.8	89.1
	(−9.11)	(9.29)	(13.14)	(3.48)		(−3.18)	(3.29)	(−4.41)			76.3	110
Mean	−18.989	2.543			0.883	1.089					95.2	94.7
	(−7.13)	(11.63)			(24.13)	(2.19)					91.1	45.2

of the explanatory variables are indicated in Table 2. Values of the explanatory variable "Padd" and of the flow metrics 0.50, 0.60, 0.70, 0.80, 0.90, 0.95 and Min (Table 3) should be incremented by 1 for inclusion in Eq. (1) (cf. Section 2). As examples, Eqs. (6) and (7) show how to predict the 0.95 flow percentile ($Q_{0.95}$) and mean annual flow (Q_{mean}) using the coefficients provided in Table 3.

$$Q_{0.95} = \exp^{-27.857} \times Rain^{2.698} \times Peri^{1.436} \times Elev^{0.966} \times Lati^{-1.291} \times (Padd + 1)^{-0.285} - 1 \quad (6)$$

$$Q_{mean} = \exp^{-18.989} \times Rain^{2.543} \times Area^{0.883} \times Drai^{1.089} \quad (7)$$

In order to make the power-law models usable by a broad range of users, Table 3 presents, for each of the 14 flow metrics, an equation including climatic, geomorphologic and/or geographic explanatory variables only, exclusive of other catchment characteristics. This way, users with access to the DEM and the rainfall database only, can predict the flow metrics and derive FDCs at any point along the Lower Mekong tributaries. A second equation is provided for the flow metrics which are better predicted with an additional explanatory variable related to land cover. Except the $Q_{0.95}$ model whose predictive power is greatly improved by the inclusion of paddy area as an explanatory variable, *R*-squared increments for the other models are modest. It should be noted that the predictive power of all models may reduce if they are applied to catchments with characteristics outside the range of values reported in Table 2.

Drainage directions, soil characteristics, longitude and wetland areas were found not to have significant explanatory power for any of the flow metrics. These exclusions do not necessarily mean that the mentioned variables have no effect on the catchments' hydrological behavior. For instance, the hydrological effects of soils and wetlands are complex and depend on various context-specific situations (Ribolzi et al., 2011; Acreman and Holden, 2013) which may not be reflected by the available metrics that we used. In addition, it should be noted that the surface area of wetlands never exceeds 1.23% of the catchment areas, for the catchments used in the analyses. This likely explains their negligible role in hydrological responses.

Annual rainfall is an explanatory variable in all models with associated coefficients exhibiting the lowest variability between models (variation coefficient < 10%). Values are much greater than unity (average = 2.59) indicating that an increase of *x*% in annual rainfall would induce an >*x*% increase in any of the studied flow metrics. The rainfall coefficient associated to the model predicting mean annual flow ($\beta_1 = 2.543$) corresponds to the rainfall elasticity of streamflow. It is greater than the value 1.99 obtained by Hapuarachchi et al. (2008) for the whole Mekong Basin. These elasticity coefficients can help assess the impact of projected changes in rainfall on future changes in the studied streamflow metrics.

The drainage area is an explanatory variable for mean annual flow and high-flow variables (Max, 0.10, 0.20, 0.30 and Mean). The coefficients for this variable are slightly lower than 1, depicting a slight tendency for reduction in runoff depth as catchment size increases. This is in agreement with Pilgrim et al. (1982) who observed a tendency of increased seepage in larger catchments. In contrast, low-flow variables (0.40, 0.50, 0.60, 0.70, 0.80, 0.90, 0.95 and Min) are better explained by the catchment perimeter rather than the catchment area. The perimeter provides information related to the shape of the catchment. For a given catchment area, a greater perimeter implies a longer time for water to reach the catchment outlet, thus explaining the positive correlation with low flow variables. Further, it should be noted that the coefficients associated to the drainage area tend to decrease for higher flow metrics (i.e. lower flow percentiles), and the coefficients associated to the perimeter tend to decrease for lower flow metrics (i.e. higher flow percentiles). These behaviors could reflect the influence of the wetted areas and the water head on seepage rates during flood events and the influence of evaporation and seepage combined to the flow transit time across the catchment during low flow periods. These suppositions need to be strengthened by further research on this topic.

The drainage density quantifies the level of catchment drainage by stream channels. Lower drainage density corresponds to flatter land with less differentiated drainage paths. High values imply steeper-sided thalweg, shorter flow transfer time and a sharper hydrograph. As would be anticipated, the coefficients of the drainage density are consistently positive and negative for high flow and low flow, respectively. Flow percentiles of intermediate magnitude are not influenced by the drainage density (Table 3).

The surface ratio of paddy rice is negatively correlated to four low-flow variables (0.60, 0.70, 0.80 and 0.95). One possible explanation is the ability of paddy fields to reduce groundwater recharge due to the impermeable soil layer below the rice root zone, which contributes to the maintenance of ponded water in the bunded rice fields and increased evapotranspiration (Bouman et al., 2007).

The signs of the coefficients associated to the other explanatory variables are more difficult to explain. For instance, the positive coefficients relating to slope, for extreme high and low flows metrics only (Table 3) are difficult to interpret, corroborating the acknowledged complexity of the relationship between infiltration rate and slope steepness (Ribolzi et al., 2011). It is also difficult to interpret the majority of positive coefficients associated to the mean elevation. Strikingly, latitude is negatively correlated to virtually all low flow variables above the 0.50 percentile. It is tempting to conclude that latitude is a surrogate for an environmental variable controlling flow production, not listed in Table 2, and exhibiting a latitudinal gradient. However, at this stage, it is not possible to provide a candidate explanation for this particular behavior. The nature of the causal link between increased forest coverage and greater median flow (50%) (cf. the positive coefficient in Table 3) is also questionable and could be interpreted in many ways. Given the complex relationship between tropical forest and hydrology (Bruijnzeel, 2004), it is wiser not to provide a physical explanation without further research.

Table 3 shows that R^2_{adj} and R^2_{pred} values are excellent (>90%) for most of the variables. According to the *t*-ratio values reported in Table 3, the predictors with the greatest explanatory power are "drainage area" or "perimeter", depending on the predicted flow metrics. Given that the values of these two variables span over several orders of magnitude (Table 2), the high values of R^2_{adj} and R^2_{pred} reported in Table 3 could be largely attributed to mass balance considerations. In other words, these high values could simply indicate that a much larger catchment is producing much more flow. To verify if this scale issue actually magnifies the performance of the models, we re-performed the multiple regression analyses using specific runoff (in $m^3\ s^{-1}\ km^{-2}$) as dependent variables and computed NSE based on volumetric runoff for the two sets of power-law models predicting either specific or volumetric runoff. According to this efficiency coefficient, the models predicting specific runoff were found not to outperform those described in this paper and are therefore not reported here.

Except for the model predicting maximum daily flow which has one of the lowest values for R^2_{pred}, the models predicting the higher half of the FDC ($0.05 \leq$ flow percentiles ≤ 0.60), have a mean R^2_{pred} (92.97%) higher than that (90.41%) of the models predicting the lower half of the FDC ($0.70 \leq$ flow percentiles ≤ 0.95 and "Min"). This comparison only considers the best model (highest R^2_{pred}) for each flow metric (Table 3). The better prediction of high flow, compared to low flow, suggests that the explanatory variables tested in this analysis (mainly geomorphological and climate characteristics) do not correspond to the catchment characteristics that predominantly control low flows. Similar contrast between the predictive power of high-flow and low-flow models has been observed under various hydrological conditions (Thomas and Benson, 1970), suggesting that more efforts are needed to generate catchment characteristics suitable for multivariate low flow predictions.

Fig. 2 illustrates this contrast in performance by comparing observed ($Q_{j,obs}$) and predicted ($Q_{j,pred}$) flow in each studied catchment *j* for mean annual flow (Fig. 2a and c) and for the model predicting the 0.95 flow percentile with the best performance (Fig. 2b and d). Runoff values are volumetric ($m^3\ s^{-1}$) in Fig. 2a and b and specific ($m^3\ s^{-1}\ km^{-2}$) in Fig. 2c and d. The NSE values calculated with volumetric runoff (Fig. 2a and b) are greater than those obtained with specific runoff (Fig. 2c and d), reflecting the mass balance effect (i.e. larger catchments produce more flow) explained above. Although the scatter plots in Fig. 2a and b align well along the first bisector, 30% and 50% of the catchments, respectively, have an absolute normalized error (ANE_j for catchment *j*, Eq. (8)) greater than 40%. These errors result from the assumptions of the modeling method and from possible inaccuracies in the original flow values used in the model parameterization. Even though cross-validation has been performed, extrapolation to ungauged catchments still adds non-measurable uncertainty. Therefore, we encourage users of these models to cross check predicted flow with other flow prediction methods, if they are available.

$$ANE_j = \left| \frac{Q_{j,pred} - Q_{j,obs}}{Q_{j,obs}} \right| \tag{8}$$

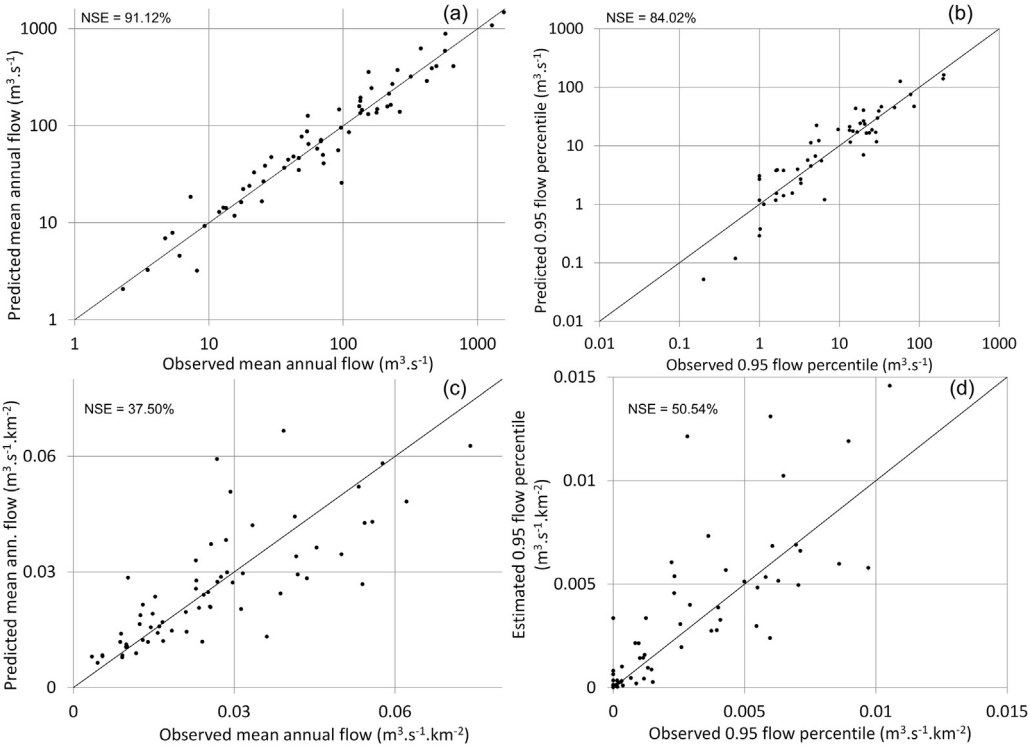

Fig. 2. Comparison of observed and predicted flows for the power-law models predicting mean annual flow (a–c) and the 0.95 flow percentile (b–d). a and b: Volumetric runoff. c and d: Specific runoff.

Fig. 3 illustrates how ANE varies according to the aridity index and the drainage area of the studied catchments for the same models used in Fig. 2. ANE is not sensitive to the flow unit (either specific or volumetric runoff). The aridity index is the ratio between mean annual potential evapotranspiration and mean annual rainfall computed using the Climate Research Unit data from Harris et al. (2014). This index varies between 0.26 and 0.64 with a median of 0.45. This range is similar to that of the wettest regions in other parts of the world where similar regression models have been developed (cf. the syntheses of Salinas et al., 2013 and of Blöschl et al., 2013). These authors show that the regressions models with the lowest ANE values (i.e. best predictive performance) correspond to these wettest regions. Where aridity increases, flow prediction is hampered by greater hydrological variability and higher presence of intermittent rivers. The ANE values of the annual flow model reported in this paper (Fig. 3a) are similar to those observed in other regions under the same aridity conditions (cf. Fig. 5.27 in Blöschl et al., 2013). The ANE values of the 0.95 flow percentile model reported in this paper (Fig. 3b) are slightly greater than those observed in other regions under the same aridity conditions (Fig. 5 in Salinas et al., 2013).

In their Fig. 5, Salinas et al. (2013) show that the ANE of low flow models is lower in larger catchments. The authors explain this by the greater space-time aggregation of runoff processes in larger catchments, increasing the predictability. In contrast, no correlation between ANE and the drainage area is observed in our analysis (Fig. 3c and d). This absence of trend is expected for the model predicting mean annual flow (Fig. 3c) which includes drainage area as an explanatory variable (Table 3), confirming the homoscedasticity of the residuals in Eq. (2). This explanation remains valid for the model predicting the 0.95 flow percentiles (Fig. 3d) for the two following reasons: (i) the catchment perimeter is the main predictor for this model; (ii) the logarithmic forms of the drainage area and perimeter of the studied catchments are highly correlated: $R^2 = 0.97$.

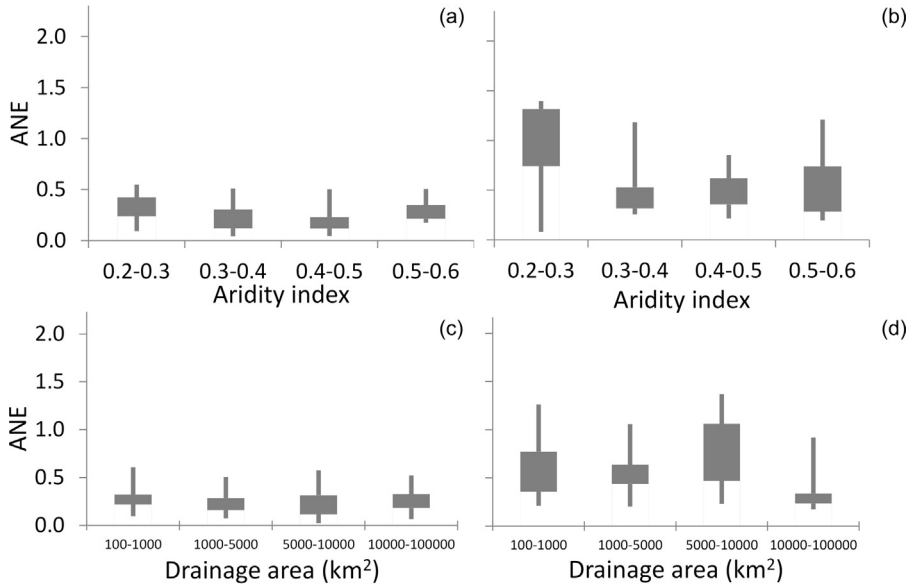

Fig. 3. Absolute normalized error (ANE) of predicting mean annual flow (a and c) and the 0.95 flow percentile (b and d) as a function of aridity index and drainage area. Boxes are 40–60% quantiles, whiskers are 20–80% quantiles.

ANE allows the predictive performance of the models to be assessed on an individual catchment basis and to determine how it relates to the catchments characteristics. In contrast, R^2_{adj}, R^2_{pred}, NSE and RMSNE enable an assessment of how well the models described in this paper perform, compared to regional regression models developed in other parts of the world. For example, the values of R^2_{pred} and R^2_{adj} for the model predicting annual flow (Table 3), were compared with the squared correlation coefficients based on volumetric runoff of the annual flow models compiled by Blöschl et al. (2013) (Fig. 5.26 in their review), and show similar good performances. The low aridity index of the Lower Mekong Basin may contribute to this good performance as previously discussed. The goodness of fit of the low flow models (Table 3) were compared with that of the low flow models included in the comparative assessment of Salinas et al. (2013). This comparison is only approximate because the definitions of low flow in the studies compiled by Salinas et al. (2013) are not strictly equivalent to our definitions. In addition, the benchmark produced by Salinas et al. (2013) for low flow models (cf. their Fig. 3, left panel) only includes R^2 values (equivalent to NSE) based on specific runoff. Therefore, we recomputed NSE coefficients for our "Min" and "0.95" models using specific runoff and obtained the values 28.4% and 50.5%, respectively, which are lower than the range of values plotted by Salinas et al. (2013). This comparison indicates that the low flow models "Min" and "0.95" are more suited for volumetric runoff prediction. The performance of the high flow models "Max" (RMSNE = 71.5%) and "0.05" (RMSNE = 53.1%) was compared with the baseline provided by Salinas et al. (2013) who used RMSNE to assess the predictive performance of the reviewed high flow models (cf. their Fig. 3, right panel). "Max" and "0.05" were found to perform better than 25% and 50% of the models reviewed by Salinas et al. (2013). While RMSNE is not sensitive to the flow unit (either specific or volumetric runoff), this comparison is only indicative, again, because the definitions of the high flow variables reviewed by Salinas et al. (2013) differ from our definitions.

5. Conclusions

The primary goal of this study was to provide a system of simple equations to estimate streamflow metrics at any point along the tributaries of the Lower Mekong River, from easily obtained climatic

and geomorphologic characteristics. Multivariate power-law models were found to perform well, with prediction R-squared ranging from 89.09 to 94.71% for the best models predicting each flow metric. The prediction of most of the low-flow metrics was slightly improved by the inclusion of forest cover or paddy cover as explanatory variables, suggesting a causal link between these land-cover types and low flow hydrology. In addition to flow prediction, these multivariate power law models can be used for a range of applications: prediction of climate change impact on mean, low and high basin water yields, assessment of the effect of paddy area expansion on low flow, regional impact assessment of local hydrological alterations through the comparison of water yields from nested basins.

Conflict of interest

None declared.

Acknowledgments

This study was funded by the Water, Land and Ecosystems CGIAR research program and the United Nations Environment Programme. These sponsors had no role in the study design, in the collection, analysis and interpretation of the data, in the writing of the report and in the decision to submit the article for publication. The authors are grateful to the Mekong River Commission, particularly Thanapon Piman, for the provision of streamflow data, the land-cover map and the soil data, to the project members of APHRODITE's Water Resources for the provision of the rainfall data base, and to USGS HydroSHEDS for the provision of the digital elevation model. The authors thank the reviewer of an earlier version of this paper, Alberto Viglione, for the helpful suggestions and constructive comments.

References

Acreman, M., Holden, J., 2013. How wetlands affect floods. Wetlands 33, 773–786.
Arias, M.E., Cochrane, T.A., Piman, T., Kummu, M., Caruso, B.S., Killeen, T.J., 2012. Quantifying changes in flooding and habitats in the Tonle Sap Lake (Cambodia) caused by water infrastructure development and climate change in the Mekong Basin. J. Environ. Manage. 112, 53–66.
Blöschl, G., Sivapalan, M., Wagener, T., Viglione, A., Savenije, H., 2013. Runoff Prediction in Ungauged Basins. Synthesis Across Processes, Places and Scales. University Press, Cambridge.
Bouman, B.A.M., Humphreys, E., Tuong, T.P., Barker, R., 2007. Rice and water. Adv. Agron. 92, 187–237.
Bruijnzeel, L.A., 2004. Hydrological functions of tropical forests: not seeing the soil for the trees? Agric. Ecosyst. Environ. 104, 185–228.
Castellarin, A., Botter, G., Hughes, D.A., Liu, S., Ouarda, T.B.M.J., Parajka, J., Post, D.A., Sivapalan, M., Spence, C., Viglione, A., Vogel, R.M., 2013. Prediction of flow duration curves in ungauged basins. In: Blöschl, G., Sivapalan, M., Wagener, T., Viglione, A., Savenije, H. (Eds.), Runoff Prediction in Ungauged Basins: Synthesis Across Processes, Places and Scales. University Press, Cambridge, pp. 135–162.
Castellarin, A., Galeati, G., Brandimarte, L., Montanari, A., Brath, A., 2004. Regional flow-duration curves: reliability for ungauged basins. Adv. Water Resour. 27, 953–965.
Cook, R.D., Weisberg, S., 1982. Residuals and Influence in Regression. Chapman and Hall, New York.
Hapuarachchi, H.A.P., Takeuchi, K., Zhou, M., Kiem, A.S., Georgievski, M., Magome, J., Ishidaira, H., 2008. Investigation of the Mekong River basin hydrology for 1980–2000 using the YHyM. Hydrol. Process. 22, 1246–1256.
Harris, I., Jones, P.D., Osborn, T.J., Lister, D.H., 2014. Updated high-resolution grids of monthly climatic observations – the CRU TS3.10 Dataset. Int. J. Climatol. 34, 623–642.
Helsel, D.R., Hirsch, R.M., 2002. Statistical Methods in Water Resources. US Geological Survey, Reston, VA.
Homa, E.S., Brown, C., McGarigal, K., Compton, B.W., Jackson, S.D., 2013. Estimating hydrologic alteration from basin characteristics in Massachusetts. J. Hydrol. 503, 196–208.
Johnston, R., Kummu, M., 2012. Water resource models in the Mekong Basin: a review. Water Resour. Manage. 26 (2), 429–455.
Kingston, D.G., Thompson, J.R., Kite, G., 2011. Uncertainty in climate change projections of discharge for the Mekong River Basin. Hydrol. Earth Syst. Sci. 15, 1459–1471.
Lehner, B., Verdin, K., Jarvis, A., 2006. HydroSHEDS Technical Documentation. World Wildlife Fund US, Washington, DC.
MRC, 2011. Planning Atlas of the Lower Mekong River Basin. Basin Development Plan Programme. Mekong River Commission (MRC), Vientiane, Phnom Penh.
Osti, R., Hishinuma, S., Miyake, K., Inomata, H., 2011. Lessons learned from statistical comparison of flood impact factors among southern and eastern Asian countries. J. Flood Risk Manage. 4 (3), 203–215.
Pech, S., Sunada, K., 2008. Population growth and natural-resources pressures in the Mekong River Basin. Ambio 37 (3), 219–224.
Pilgrim, D.H., Cordery, I., Baron, B.C., 1982. Effects of catchment size on runoff relationships. J. Hydrol. 58, 205–221.
Ribolzi, O., Patin, J., Bresson, L.M., Latsachack, K.O., Mouche, E., Sengtaheuanghoung, O., Silvera, N., Thiébaux, J.P., Valentin, C., 2011. Impact of slope gradient on soil surface features and infiltration on steep slopes in northern Laos. Geomorphology 127, 53–63.

Salinas, J.L., Laaha, G., Rogger, M., Parajka, J., Viglione, A., Sivapalan, M., Blöschl, G., 2013. Comparative assessment of predictions in ungauged basins – Part 2. Flood and low flow studies. Hydrol. Earth Syst. Sci. 17, 2637–2652.
Tasker, G.D., 1980. Hydrologic regression with weighted least squares. Water Resour. Res. 16 (6), 1107–1113.
Thomas, D.M., Benson, M.A., 1970. Generalization of Streamflow Characteristics from Drainage-Basin Characteristics. USGS, Washington, Water-supply paper 1975.
Vogel, R.M., Fennessey, N.M., 1994. Flow-duration curves. I: New interpretation and confidence intervals. J. Water Resour. Plan. Manage. 120 (4), 485–504.
Vogel, R.M., Wilson, I., Daly, C., 1999. Regional regression models of annual streamflow for the United States. J. Irrig. Drain. Eng. 125 (3), 148–157.
Yatagai, A., Kamiguchi, K., Arakawa, O., Hamada, A., Yasutomi, N., Kitoh, A., 2012. APHRODITE: constructing a long-term daily gridded precipitation dataset for Asia based on a dense network of rain gauges. Bull. Am. Meteorol. Soc. 93 (9), 1401–1415.
Ziv, G., Baran, E., Nam, S., Rodriguez-Iturbe, I., Levin, S.A., 2012. Trading-off fish biodiversity, food security, and hydropower in the Mekong River Basin. Proc. Natl. Acad. Sci. U. S. A. 109 (15), 5609–5614.